Exp. Anim. 65(3), 311–318, 2016

—Original—

Tracking cells implanted into cynomolgus monkeys (*Macaca fascicularis*) using MRI

Yasuyo ITO-FUJISHIRO[1,2], Hiroshi KOIE[2], Hiroaki SHIBATA[1], Sachi OKABAYASHI[3], Yuko KATAKAI[3], Chieko OHNO[3], Kiichi KANAYAMA[2], Yasuhiro YASUTOMI[1,4], and Naohide AGEYAMA[1]

[1]*Tsukuba Primate Research Center, National Institutes of Biomedical Innovation, Health and Nutrition, Hachimandai 1-1, Tsukuba, Ibaraki 305-0843, Japan*
[2]*College of Bioresource Sciences, Nihon University, Japan*
[3]*The Corporation for Production and Research of Laboratory Primates, Japan*
[4]*Mie University Graduate School of Medicine, Department of Molecular and Experimental Medicine, Japan*

Abstract: Regenerative therapy with stem cell transplantation is used to treat various diseases such as coronary syndrome and Buerger's disease. For instance, stem-cell transplantation into the infarcted myocardium is an innovative and promising strategy for treating heart failure due to ischemic heart disease. Basic studies using small animals have shown that transplanted cells improve blood flow in the infarcted region. Magnetic resonance imaging (MRI) can noninvasively identify and track transplanted cells labeled with superparamagnetic iron oxide (SPIO). Although clinical regenerative therapies have been clinically applied to patients, the fate of implanted cells remains unknown. In addition, follow-up studies have shown that some adverse events can occur after recovery. Therefore, the present study evaluated the ability of MRI using a 3T scanner to track implanted peripheral blood mononuclear cells labeled with SPIO on days 0 and 7 after intramuscular (i.m.) and intravenous (i.v.) injection into a cynomolgus monkey. Labeled cells were visualized at the liver and triceps surae muscle on MR images using T1- and T2-weighted sequences and histologically localized by Prussian blue staining. The transplanted cells were tracked without abnormal clinical manifestations throughout this study. Hence, MRI of cynomolgus monkey transplanted SPIO-labeled cells is a safe and efficient method of tracking labeled cells that could help to determine the mechanisms involved in regenerative therapy.

Key words: MRI, nonhuman primate, stem cells

Introduction

Regenerative medicine based on stem cell transplantation has been applied in efforts to treat ischemic diseases such as myocardial infarction, angina pectoris, Buerger's disease, and chronic arteriosclerosis obliterans. Presently 500,000–800,000 and 10,000–12,000 patients in Japan have arteriosclerosis obliterans (ASO) and Buerger's disease, respectively. Patients with peripheral artery ischemia in all four limbs require quadruple amputation if surgery and medical therapy are ineffective. Vascular regenerative therapies have recently attracted interest as a means of improving the quality of life of such patients. Cardiovascular cell tracking studies are presently being implemented at the preclinical stage, whereas the number of clinical trials of

(Received 17 December 2015 / Accepted 15 March 2016 / Published online in J-STAGE 11 April 2016)
Address corresponding: N. Ageyama, Tsukuba Primate Research Center, National Institutes of Biomedical Innovation, Health and Nutrition, Hachimandai 1-1, Tsukuba, Ibaraki 305-0843, Japan
Abbreviations: MRI, magnetic resonance imaging; PBMCs, peripheral blood mononuclear cells; SPIO, superparamagnetic iron oxide

stem cell therapies is rapidly increasing. Some preliminary human trials of stem cell therapy have delivered promising results in terms of treating left ventricular dysfunction that arises after myocardial infarction and using MRI to assess outcomes [8, 10, 22]. However, others have been less positive [14, 17]. According to the Trans-Atlantic Inter-Society Consensus Document on Management of Peripheral Arterial Disease (TASC) [7] and TASCII, therapeutic angiogenesis and/or regenerative therapy have been carried out at several facilities by transplanting autologous cells derived from bone marrow. Insurance coverage for such therapy was approved in 2003 to treat ASO and Buerger's disease [25]. Unfortunately, regenerative therapy is currently only available to patients who satisfy the selection criteria for a likely cure as judged by the hospital that they attend. Although the selection criteria are adequate, follow-up studies have shown that adverse events such as exacerbation of cutaneous ulceration, pain at rest, and sudden death can occur after the area affected by Buerger's disease is improved [17, 25]. Basic studies using small animals have shown that transplanted cells improve blood flow in regions of infarction [5, 24]. One approach to understanding the mechanism of the improvement induced by regenerative medicine is to track magnetically-labeled transplanted cells using magnetic resonance imaging (MRI) [11, 16], and another is to detect cells after transplantation using superparamagnetic iron oxide (SPIO) and/or MRI [26]. However, such studies have not yet been implemented in humans or other large animal species, which might be far more appropriate preclinical models than small animals. Among large animals, nonhuman primates should be excellent models because of their close phylogenetic relationship to humans [1, 15, 27]. Although there is some disapprobation, labeling with SPIO does not exert short or long-term toxic effects on tumors or normal cells [22, 30]. Ferumoxide (Feridex) and ferucarbotran (Resovist) are included in SPIO used in MRI analyses [3, 9]. These agents distort the magnetic field, shorten the T2 relaxation time, and generate signal voids (black spots) in T2-weighted MR images. The major differences between them are the concentration of iron in the stock solution (11.2 vs. 0.45 mg Fe/ml) and particle size (120–180 vs. ~60 nm) [29]. Feridex labels murine macrophage-like cells via receptor-mediated endocytosis [20, 21]. Here we determined and applied the optimal SPIO concentration required to label cells. We then used 3T MRI to track labeled cells at days 0 and 7 at the gastrocnemius muscle and liver after transplantation, respectively. We compared the data obtained from tracking the labeled cells to identify the spontaneous disappearance of SPIO after implantation. As mentioned above, we used two types of SPIO, Feridex and Resovist, to label peripheral blood mononucleated cells. Because of the bigger size and better Prussian blue stainability of Feridex than Resovist, we mixed cells labeled with Feridex and Resovist to maximize SPIO signals on MR images before injection into cynomolgus monkey. We also analyzed the survival rates of cells labeled with Feridex and Resovist individually before mixing the two to identify the effect of particle size on cell damage. Finally, we established a way to track transplanted cells in cynomolgus monkeys and evaluate the safety and efficacy of regenerative medicine using MRI and SPIO.

Materials and Methods

Animals

The present study utilized 5-year-old mature male cynomolgus monkey that weighed 4.5 kg and had been bred and maintained at the Tsukuba Primate Research Center (Ibaraki, Japan). This study proceeded according to the Rules for Animal Care and Management of Tsukuba Primate Center [13] and the Guiding Principles for Animal Experiments Using Nonhuman Primates formulated by the Primate Society of Japan [19]. The Animal Welfare and Animal Care Committee of the National Institutes of Biomedical Innovation, Health and Nutrition (NIBIOHN, Osaka, Japan) approved the experimental protocol. All animal facilities had individualized but comparable protocols for inducing anesthesia in nonhuman primates [28]. We collected peripheral blood mononuclear cells (PBMCs) from the monkey under general anesthesia induced by ketamine hydrochloride (Ketalar, 10 mg/kg; i.m.) (Sankyo, Tokyo, Japan) as described previously [2].

Isolation of PBMCs and labelling with SPIO particles

Peripheral blood mononuclear cells isolated from whole blood were purified by density gradient centrifugation using Ficoll-Paque (Amersham Biosciences) as described for bone marrow cells [23] and washed twice with phosphate-buffer saline (PBS). The cells were hemolyzed at 37°C for a few mins using ammonium chloride-potassium lysis buffer (ACK), washed, and brought to a density of 1×10^7/ml. The cells were then

cultured and maintained in RPMI1640 (Wako Pure Chemical Industries, Ltd., Osaka, Japan) with 10% fetal bovine serum (FBS; Biosource, Rockville, MD, USA) supplemented with 0.1 mg/ml streptomycin (Meiji Seika Co., Tokyo, Japan) and 100 U/ml penicillin (Banyu Pharmaceutical Co., Tokyo, Japan) in six-well plates at 37°C under a 5% CO_2 atmosphere. Cells (1×10^7/ml medium) were labeled with 100%, 10%, 1%, and 0.1% ratios of each SPIO stock solution for 12 h. Viability and the concentrations of ferucarbotran (Resovist, Bayer Schering Pharma, Berlin, Germany, http://www.bayerhealthcare.com) and ferumoxide (Feridex I.V., AMAG Pharmaceuticals, Lexington, MA, USA; http://www.amagpharma.com) were measured as described below. Feridex- and Resovist-labeled PBMCs were mixed and washed in PBS, trypsinized, washed, and resuspended in PBS. Finally, 5.5×10^7 and 6.6×10^6 PBMCs/ml were respectively labeled with Resovist and Feridex.

Staining methods, cell viability, and SPIO content

After SPIO labeling, PBMCs were washed, and then the cell viability and SPIO content were measured to assess the efficiency of the labeling and to histologically compare Feridex and Resovist labeling using Trypan blue staining of cultured cells and Prussian blue staining [9] of cytospin specimens that were fixed with 4% paraformaldehyde for 15 min. The specimens were incubated for 30 min with 2% potassium ferrocyanide in 2% hydrochloric acid and counterstained with nuclear fast red to visualize intracellular SPIO and cell profiles. When the cells stained positive for Prussian blue, SPIO appeared as blue intracellular precipitates. We then compared viability of PBMCs labeled with Feridex and Resovist and the ratio of the iron content. We established the final labeling of Feridex and Resovist concentrations based on the findings of these procedures. Cell viability was determined before injecting them into the monkey.

Transplantation

After SPIO labeling for 12 h, we transplanted the labeled PBMCs. To avoid the destruction of implanted cells caused by the injection pressure and tight junctions of myocytes, we decided to inject all the labeled cells in small amounts at each site separately but as closely together as possible. Four regions of the gastrocnemius of cynomolgus monkey were transplanted i.m. with a 1-ml suspension of 2.7×10^7 SPIO-labeled PBMCs using a 22-gauge needle. Thereafter, an 11-ml suspension of 2.7×10^8 PBMCs was injected into the saphenous vein using a 22-gauge intravenous cannula (Terumo, Tokyo, Japan). The administered volume of cells was increased by mixing the PBMCs labeled with the two types of SPIOs. These procedures were accomplished under general anesthesia that was induced with ketamine hydrochloride (Ketalar, 10 mg/kg; Sankyo, Tokyo, Japan) as described above and maintained with isoflurane (Aestiva/5; GE Healthcare, Madison, WI, USA). The monkey exhibited no clinical signs or symptoms after transplantation.

MR imaging

Transplanted cells labeled with SPIO can be noninvasively identified and tracked using MRI. We compared MR images acquired from transplanted monkey using a 3T MR scanner (Magnetom Allegra; Siemens, Erlangen, Germany) on days 0 and day 7 with those acquired before transplantation. Monkey was placed in the dorsal position with a head coil, and anesthesia was maintained with ketamine hydrochloride and isoflurane during assessment by 3T MR using ECG and respiratory gating. T1- and T2-weighted images were acquired using the following parameters: TR, 4000; TE, 18; field of view, 180*180; slice thickness, 700 μm.

Histological analysis

After acquiring the MR imaging on day 7, a monkey was deeply anaesthetized with a lethal dose of sodium pentobarbital. Tissue samples of the gastrocnemius muscle and liver were obtained by necropsy. Those tissues were fixed in 10% neutral buffered formalin, processed routinely, and embedded in paraffin wax. Sections (4 μm) were deparaffinized and stained with Prussian blue to assess Feridex and Resovist labeling in PBMCs. We also performed immunostaining of transplanted cells. Sections were incubated free floating in anti-CD68 mouse monoclonal antibody solution (clone KP1, Dako; 1 in 100 dilution) at 4°C overnight. Following brief washes with a buffer, the sections were sequentially incubated with biotinylated goat anti-mouse IgG, followed by streptavidin-alkaline phosphatase (Dako).

Results

Viability of labeled cells

First of all, we verified that there were no differences in the viabilities with labeled and non-labeled cells, and the viability of the labeled cells was>90% regardless of

Table 1. Viability of labeled cells depends on the type and concentration of SPIO

SPIO type	SPIO (mg Fe/ ml)	Ratio (%) of stock solution (/ml medium)	Viability
Feridex	2.8	10%	92.4%
	0.28	1%	95.2%
	0.028	0.1%	95.1%
Resovist	2.7	10%	98.7%
	0.27	1%	94.8%
	0.027	0.1%	92.1%

SPIO, superparamagnetic iron oxide.

the Feridex and Resovist concentrations (Table 1). The SPIO concentration of 1% stock solution/ml of medium generated clear images of SPIO-labeled phagocytized cells. Cell viability did not differ between the two types of SPIO, although cells labeled with Feridex using cytospin were exceptionally clear. Figures 1A and 1B show images of PBMCs labeled with 1% Feridex and 1% Resovist. Feridex particles are larger than Resovist particles. We therefore considered that a 1% stock solution/ml of these particles was optimal. Cells were co-incubated with SPIO and then injected into cynomolgus monkey.

Tracking labeled PBMCs with MRI

We injected 2.7×10^7 and 2.7×10^8 PBMCs labeled with Feridex and Resovist into the triceps surae muscle and saphenous vein, respectively, of the monkey and then assessed the location of the cells using MRI on days 0 and 7. Throughout Figs. 2 and 3, we regarded the left triceps surae muscle as the control for the pre-injected state. This is because we ensured that we injected the labeled cells into the muscles directly without any backward flow of blood and there is an extremely low possibility that the labeled cells flow into blood vessels by intramuscular injection. Figures 2A and 2C and 3A show T1- and T2-weighted images, respectively, of the long axis of the triceps surae muscle on day 0. Figures 4A and 4B shows T1- and T2-weighted images of the short axis of the liver soon after injection on day 0. In addition, Figs. 4C and 4D shows T1- and T2-weighted images of injected non-labeled cells in the same position. White arrows show SPIO signals from PBMCs indicating the remains of implanted, labeled cells. Figures 2B and 2D and 3B show T1- and T2-weighted images, respectively, of the triceps surae muscle at 7 days after injection. The intensity of the SPIO signals in the muscle remained unchanged at the same site when compared with the intensity on day 0. However, MRI did not detect any signals from the liver at 7 days after injection (data not shown).

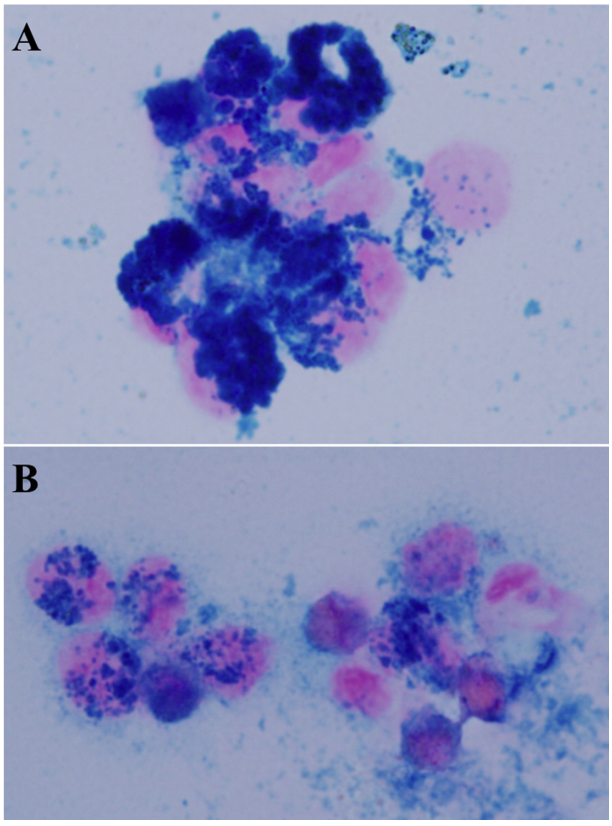

Fig. 1. Peripheral blood mononuclear cells labeled with SPIO and visualized by microscopy. Feridex (A) and Resovist (B) labeling (magnification, × 1,000). Blue spots in pink regions indicate magnetically-labeled nuclei stained with Prussian blue. Feridex particles are larger than Resovist particles. SPIO, superparamagnetic iron oxide.

Histopathological analysis

Microscopically, some labeled cells stained with Prussian blue were observed in the triceps surae muscle as the blue accumulation spot (Fig. 5), and these cells were identified as macrophages by CD68 immunostaining (data not shown); thus they indicated the remains of transplanted cells labeled by the iron particles of SPIO. We verified the remains of labeled cells as Prussian blue-positive cells not only at the site of the triceps surae but also in the right lateral segment of the liver, though there were no accumulation spots in the liver (data not shown).

Fig. 2. T1-weighted MR images of the long axis (A and B) and transverse (C and D) of the triceps surae muscle. Days 0 (A and C) and 7 (B and D) after transplantation. Black spots with white arrows indicate magnetic labeling as negative contrast. MR, magnetic resonance.

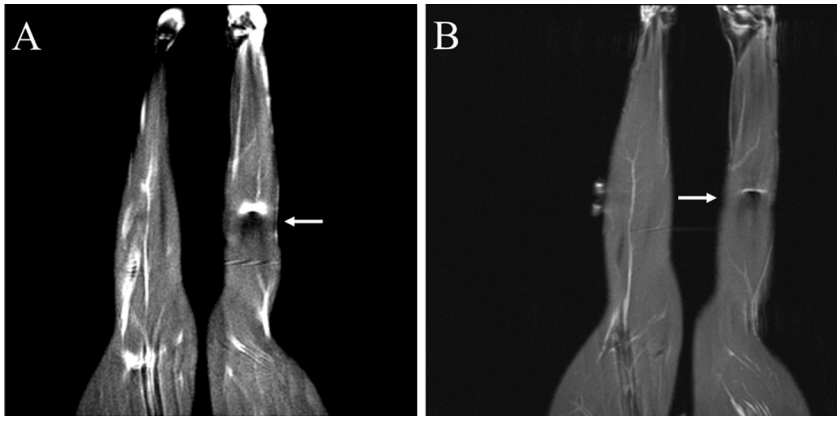

Fig. 3. T2-weighted MR images of the long axis of the triceps surae muscle. Days 0 (A) and 7 (B) after transplantation. Black spots with white arrows indicate magnetic labeling as negative contrast. MR, magnetic resonance.

Discussion

The harmful effects of SPIO have been debated [4, 22, 30]. We found here that two types SPIO were not cytotoxic and that the experimental monkey did not develop any clinical signs or symptoms throughout the study. MR imaging of the triceps surae muscle on day 7 showed that clear SPIO signals still remained. Though

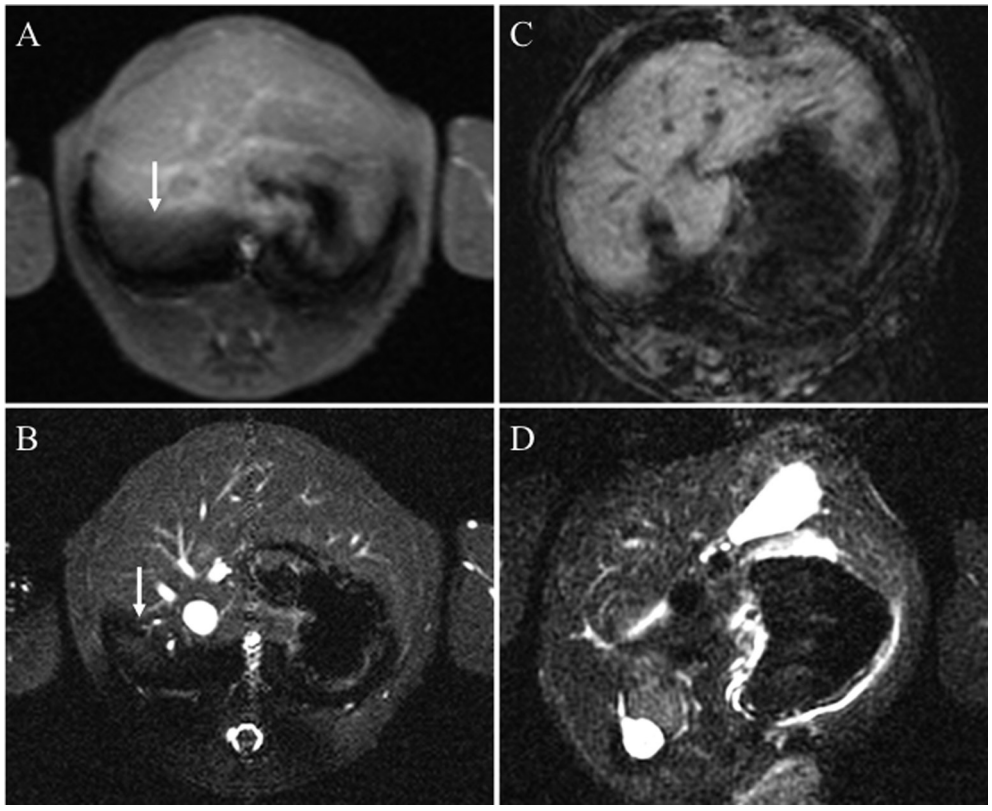

Fig. 4. T1- and T2-weighted MR images of the short axis of the liver shortly after injection into the saphenous vein on day 0 (A and B, respectively) and images of non-labeled injected cells (C and D, respectively). White arrows show SPIO signals. MR, magnetic resonance.

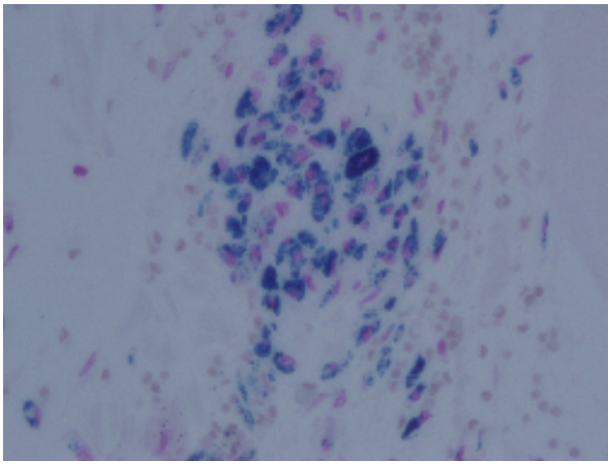

Fig. 5. Remains of SPIO in macrophages at the triceps surae muscle (magnification, × 400). Blue spots indicate residues of labeled cells after injection i.m. SPIO, superparamagnetic iron oxide.

the black spots of some injections became ambiguous, the edges of the spots were still clearly visible. It is possible to visualize the accumulated and engrafted and/or scarred implanted SPIO-labeled cells because an MRI scanner can catch the signals of a small amount of SPIO. The MR image of the external side of the right hepatic lobe on day 7 indicated that cellular migration might be one factor affecting the disappearance of the SPIO signals from implanted cells, though the MR image of the triceps surae muscle did not show a decrease in SPIO signals compared with day 0. That is to say, transplantation intramuscularly might result in more implanted cells remaining than transplantation intravenously. Although histopathological analysis also showed a few Prussian blue-positive cells in the liver on day 7 on MRI, we could not determine whether the cells were implanted cells or endogenous iron. The possibility of distinguishing implanted cells from endogenous iron in hepatocytes and Kupffer's cells is the subject of future research. These findings, however, indicated that cells implanted i.v. might not reach targeted areas such as the liver, because they might become trapped and rejected as foreign matter. We therefore inferred that i.v. implantation of cells would not be useful as a regenerative medicine approach

because of such trapping by various organs. Injecting stem cells directly into a targeted site would be more effective than transvenous delivery for clinical applications. In addition, allograft transplantation is suitable for preclinical studies in nonhuman primates because even patients who have disorders of the hematopoietic system can receive this treatment. However, it has the demerit of requiring complicated procedures such as immunosuppressive therapy and MHC matching test. Therefore, we established this cell tracking system by autologous transplantation in cynomolgus monkeys. Furthermore, this autologous transplantation system could be suitable for some preclinical studies using iPS cells derived from individual patients such as in the case of personalized medicine [18, 31]. One goal of this manuscript was to provide sufficient information concerning this cell tracking system for those investigators who may need to perform cell implantation in nonhuman primates and thus require details about the methodology and outcome using a nonhuman primate model. In summary, we showed that MR imaging could noninvasively, safely, and effectively track transplanted cells labeled with SPIO in the cynomolgus monkey. Thus, the system can be used to evaluate and assess the safety and applicability of regenerative medicine techniques and help to disclose the mechanism (s) of such techniques. More trials are required to refine the protocol for regenerative medicine.

Fluorescent iron particles (FIPs) have also been tracked using MRI. Because FIPs are larger than SPIO, they should also be visualized using fluorescence and confocal fluorescence microscopy and/or FACS in addition to MRI [6, 12]. We plan to establish more novel systems to track other cell types based on MRI with FIPs to make them more clinically applicable.

Acknowledgments

The authors are grateful to Hiromi Ogawa and Hayato Narita for assistance with the clinical procedures. This work was supported by JSPS KAKENHI Grant Numbers 15K07789, 21700444 and 24615009 as well as grants from the Ministry of Health, Labour and Welfare of Japan.

References

1. Ageyama, N., Hanazono, Y., Shibata, H., Ohto, K., Ono, F., Nagashima, T., Ueda, Y., Donahue, R.E., Hasegawa, M., Ozawa, K., Yoshikawa, Y., and Terao, K. 2002. Safe and efficient methods of autologous hematopoietic stem cell transplantation for biomedical research in cynomolgus monkeys. *Comp. Med.* 52: 445–451. [Medline]
2. Ageyama, N., Kimikawa, M., Eguchi, K., Ono, F., Shibata, H., Yoshikawa, Y., and Terao, K. 2003. Modification of the leukapheresis procedure for use in rhesus monkeys (*Macaca mulata*). *J. Clin. Apher.* 18: 26–31. [Medline] [CrossRef]
3. Amado, L.C., Saliaris, A.P., Schuleri, K.H., St John, M., Xie, J.S., Cattaneo, S., Durand, D.J., Fitton, T., Kuang, J.Q., Stewart, G., Lehrke, S., Baumgartner, W.W., Martin, B.J., Heldman, A.W., and Hare, J.M. 2005. Cardiac repair with intramyocardial injection of allogeneic mesenchymal stem cells after myocardial infarction. *Proc. Natl. Acad. Sci. USA* 102: 11474–11479. [Medline] [CrossRef]
4. Arbab, A.S., Bashaw, L.A., Miller, B.R., Jordan, E.K., Lewis, B.K., Kalish, H., and Frank, J.A. 2003. Characterization of biophysical and metabolic properties of cells labeled with superparamagnetic iron oxide nanoparticles and transfection agent for cellular MR imaging. *Radiology* 229: 838–846. [Medline] [CrossRef]
5. Asahara, T., Murohara, T., Sullivan, A., Silver, M., van der Zee, R., Li, T., Witzenbichler, B., Schatteman, G., and Isner, J.M. 1997. Isolation of putative progenitor endothelial cells for angiogenesis. *Science* 275: 964–967. [Medline] [CrossRef]
6. Dick, A.J., Guttman, M.A., Raman, V.K., Peters, D.C., Pessanha, B.S., Hill, J.M., Smith, S., Scott, G., McVeigh, E.R., and Lederman, R.J. 2003. Magnetic resonance fluoroscopy allows targeted delivery of mesenchymal stem cells to infarct borders in Swine. *Circulation* 108: 2899–2904. [Medline] [CrossRef]
7. Dormandy, J.A. and Rutherford, R.B. 2000. Management of peripheral arterial disease (PAD). TASC Working Group. TransAtlantic Inter-Society Consensus (TASC). *J. Vasc. Surg.* 31: S1–S296. [Medline]
8. Fernández-Avilés, F., San Román, J.A., García-Frade, J., Fernández, M.E., Peñarrubia, M.J., de la Fuente, L., Gómez-Bueno, M., Cantalapiedra, A., Fernández, J., Gutierrez, O., Sánchez, P.L., Hernández, C., Sanz, R., García-Sancho, J., and Sánchez, A. 2004. Experimental and clinical regenerative capability of human bone marrow cells after myocardial infarction. *Circ. Res.* 95: 742–748. [Medline] [CrossRef]
9. He, G., Zhang, H., Wei, H., Wang, Y., Zhang, X., Tang, Y., Wei, Y., and Hu, S. 2007. In vivo imaging of bone marrow mesenchymal stem cells transplanted into myocardium using magnetic resonance imaging: a novel method to trace the transplanted cells. *Int. J. Cardiol.* 114: 4–10. [Medline] [CrossRef]
10. Hernández, P., Cortina, L., Artaza, H., Pol, N., Lam, R.M., Dorticós, E., Macías, C., Hernández, C., del Valle, L., Blanco, A., Martínez, A., and Díaz, F. 2007. Autologous bone-marrow mononuclear cell implantation in patients with severe lower limb ischaemia: a comparison of using blood cell separator and Ficoll density gradient centrifugation. *Atherosclerosis* 194: e52–e56. [Medline] [CrossRef]
11. Hill, J.M., Dick, A.J., Raman, V.K., Thompson, R.B., Yu, Z.X., Hinds, K.A., Pessanha, B.S., Guttman, M.A., Varney,

T.R., Martin, B.J., Dunbar, C.E., McVeigh, E.R., and Lederman, R.J. 2003. Serial cardiac magnetic resonance imaging of injected mesenchymal stem cells. *Circulation* 108: 1009–1014. [Medline] [CrossRef]

12. Hinds, K.A., Hill, J.M., Shapiro, E.M., Laukkanen, M.O., Silva, A.C., Combs, C.A., Varney, T.R., Balaban, R.S., Koretsky, A.P., and Dunbar, C.E. 2003. Highly efficient endosomal labeling of progenitor and stem cells with large magnetic particles allows magnetic resonance imaging of single cells. *Blood* 102: 867–872. [Medline] [CrossRef]
13. Honjo, S. 1985. The Japanese Tsukuba Primate Center for Medical Science (TPC): an outline. *J. Med. Primatol.* 14: 75–89. [Medline]
14. Janssens, S., Dubois, C., Bogaert, J., Theunissen, K., Deroose, C., Desmet, W., Kalantzi, M., Herbots, L., Sinnaeve, P., Dens, J., Maertens, J., Rademakers, F., Dymarkowski, S., Gheysens, O., Van Cleemput, J., Bormans, G., Nuyts, J., Belmans, A., Mortelmans, L., Boogaerts, M., and Van de Werf, F. 2006. Autologous bone marrow-derived stem-cell transfer in patients with ST-segment elevation myocardial infarction: double-blind, randomised controlled trial. *Lancet* 367: 113–121. [Medline] [CrossRef]
15. King, F.A., Yarbrough, C.J., Anderson, D.C., Gordon, T.P., and Gould, K.G. 1988. Primates. *Science* 240: 1475–1482. [Medline] [CrossRef]
16. Kraitchman, D.L., Heldman, A.W., Atalar, E., Amado, L.C., Martin, B.J., Pittenger, M.F., Hare, J.M., and Bulte, J.W.M. 2003. In vivo magnetic resonance imaging of mesenchymal stem cells in myocardial infarction. *Circulation* 107: 2290–2293. [Medline] [CrossRef]
17. Miyamoto, K., Nishigami, K., Nagaya, N., Akutsu, K., Chiku, M., Kamei, M., Soma, T., Miyata, S., Higashi, M., Tanaka, R., Nakatani, T., Nonogi, H., and Takeshita, S. 2006. Unblinded pilot study of autologous transplantation of bone marrow mononuclear cells in patients with thromboangiitis obliterans. *Circulation* 114: 2679–2684. [Medline] [CrossRef]
18. Morizane, A., Doi, D., Kikuchi, T., Okita, K., Hotta, A., Kawasaki, T., Hayashi, T., Onoe, H., Shiina, T., Yamanaka, S., and Takahashi, J. 2013. Direct comparison of autologous and allogeneic transplantation of iPSC-derived neural cells in the brain of a non-human primate. *Stem Cell Rep.* 1: 283–292. [Medline] [CrossRef]
19. Primate Society of Japan 1986. Guiding Principles for animal experiments using nonhuman primates. *Primate Rep.* 2: 111–113. [CrossRef]
20. Ralph, P., Prichard, J., and Cohn, M. 1975. Reticulum cell sarcoma: an effector cell in antibody-dependent cell-mediated immunity. *J. Immunol.* 114: 898–905. [Medline]
21. Raynal, I., Prigent, P., Peyramaure, S., Najid, A., Rebuzzi, C., and Corot, C. 2004. Macrophage endocytosis of superparamagnetic iron oxide nanoparticles: mechanisms and comparison of ferumoxides and ferumoxtran-10. *Invest. Radiol.* 39: 56–63. [Medline] [CrossRef]
22. Rogers, W.J., Meyer, C.H., and Kramer, C.M. 2006. Technology insight: in vivo cell tracking by use of MRI. *Nat. Clin. Pract. Cardiovasc. Med.* 3: 554–562. [Medline] [CrossRef]
23. Shibata, H., Hanazono, Y., Ageyama, N., Nagashima, T., Ueda, Y., Hasegawa, M., Ozawa, K., Yoshikawa, Y., and Terao, K. 2003. Collection and analysis of hematopoietic progenitor cells from cynomolgus macaques (*Macaca fascicularis*): assessment of cross-reacting monoclonal antibodies. *Am. J. Primatol.* 61: 3–12. [Medline] [CrossRef]
24. Shintani, S., Murohara, T., Ikeda, H., Ueno, T., Sasaki, K., Duan, J., and Imaizumi, T. 2001. Augmentation of postnatal neovascularization with autologous bone marrow transplantation. *Circulation* 103: 897–903. [Medline] [CrossRef]
25. Takahashi, M., Ishigatsubo, Y., Fujimoto, K., Miyamoto, M., Horie, T., Aizawa, Y., Amano, J., Minota, S., Murohara, T., Matsubara, H., and Ikeda, U. 2008. Therapeutic angiogenesis by autologous mononuclear cell implantation in patients with intractable vasculitis. *J Jpn Coll Angiol* 48: 421–424.
26. Terrovitis, J., Stuber, M., Youssef, A., Preece, S., Leppo, M., Kizana, E., Schär, M., Gerstenblith, G., Weiss, R.G., Marbán, E., and Abraham, M.R. 2008. Magnetic resonance imaging overestimates ferumoxide-labeled stem cell survival after transplantation in the heart. *Circulation* 117: 1555–1562. [Medline] [CrossRef]
27. VandeBerg, J.L. and Williams-Blangero, S. 1997. Advantages and limitations of nonhuman primates as animal models in genetic research on complex diseases. *J. Med. Primatol.* 26: 113–119. [Medline] [CrossRef]
28. Lee, V.K., Flynt, K.S., Haag, L.M., and Taylor, D.K. 2010. Comparison of the effects of ketamine, ketamine-medetomidine, and ketamine-midazolam on physiologic parameters and anesthesia-induced stress in rhesus (*Macaca mulatta*) and cynomolgus (*Macaca fascicularis*) macaques. *J. Am. Assoc. Lab. Anim. Sci.* 49: 57–63. [Medline]
29. Wang, Y.X. 2011. Superparamagnetic iron oxide based MRI contrast agents: Current status of clinical application. *Quant. Imaging Med. Surg.* 1: 35–40. [Medline]
30. Yocum, G.T., Wilson, L.B., Ashari, P., Jordan, E.K., Frank, J.A., and Arbab, A.S. 2005. Effect of human stem cells labeled with ferumoxides-poly-L-lysine on hematologic and biochemical measurements in rats. *Radiology* 235: 547–552. [Medline] [CrossRef]
31. Yokoo, N., Baba, S., Kaichi, S., Niwa, A., Mima, T., Doi, H., Yamanaka, S., Nakahata, T., and Heike, T. 2009. The effects of cardioactive drugs on cardiomyocytes derived from human induced pluripotent stem cells. *Biochem. Biophys. Res. Commun.* 387: 482–488. [Medline] [CrossRef]